One-Dimensional Orbital Excitations in Vanadium Oxides

S. Miyasaka,[1] S. Onoda,[2] Y. Okimoto,[3] J. Fujioka,[1] M. Iwama,[1] N. Nagaosa,[1,2,3,4] and Y. Tokura[1,2,3]

[1]*Department of Applied Physics, University of Tokyo, Tokyo 113-8656, Japan*

[2]*Spin Superstructure Project, ERATO, Japan Science and Technology Agency, c/o Department of Applied Physics, University of Tokyo, Tokyo 113-8656, Japan*

[3]*Correlated Electron Research Center (CERC), National Institute of Advanced Industrial Science and Technology (AIST), Tsukuba 305-8562, Japan*

[4]*CREST, Japan Science and Technology Agency, Saitama 332-0012 Japan*

(Received 7 June 2004; revised manuscript received 20 October 2004; published 24 February 2005)

The d electron orbital is a hidden but important degree of freedom controlling novel properties of transition-metal oxides. A one-dimensional orbital system is especially intriguing due to its enhanced quantum fluctuation. We present a combined experimental and theoretical study on the Raman scattering spectra in perovskite oxides $NdVO_3$ and $LaVO_3$ to prove that the quasi-one-dimensional orbital chain described by fermionic pseudospinons bears orbital excitations exchanging occupied orbital states on the neighboring sites, termed a two-orbiton in analogy with two-magnon.

DOI: 10.1103/PhysRevLett.94.076405 PACS numbers: 71.70.Gm, 71.27.+a, 75.30.–m, 78.30.–j

Perovskite transition-metal oxides offer a source of rich physics including the high temperature superconductivity [1] and the colossal magnetoresistance (CMR) [2]. In high-T_c cuprates, the quantum nature of spin is the most important issue leading to the resonating valence bond (RVB) idea by Anderson [3,4], while the orbital degrees of freedom are quenched by the layered crystal structure. The RVB idea originated from a one-dimensional (1D) quantum antiferromagnet, where a spin flip or a magnon with $S = 1$ is represented by the particle-hole excitation of fermions, i.e., *spinons,* carrying fractional spin quantum number $S = 1/2$. In CMR manganites, on the other hand, the orbital plays an important role in determining the spin-orbital-charge phase diagram as well as their excitation spectra [5]. The orbital in this system behaves semiclassically, because the strong Jahn-Teller (JT) coupling suppresses the quantum fluctuation. Hence the orbital excitation spectrum is well described as a small vibration around the ground state, which has been observed in the Raman scattering in $LaMnO_3$ [6]. Compared with these systems, perovskite-type vanadium oxide, RVO_3 ($R =$ rare-earth ions or Y) is an ideal system to study the quantum dynamics of orbitals. This is because the JT coupling energy is much less in the t_{2g} electron systems than in the e_g ones [7], and even the quasi-1D orbital system is available in a portion of the phase diagram [8,9].

RVO_3 have a $Pbnm$ orthorhombic structure with lattice constants of $a \approx b \approx c/\sqrt{2}$ at room temperature. These compounds undergo a magnetic transition from paramagnetic to C-type antiferromagnetic, as well as a G-type orbital ordering (OO) concomitant to a structural phase transition from orthorhombic to monoclinic lattice, as temperature (T) is lowered [10–13]. This pattern of the spin ordering (SO) and OO is shown in Fig. 1(a). There are two t_{2g} electrons in V^{3+}. One electron always occupies the d_{xy} orbital due to the orthorhombic distortion, which is coupled ferromagnetically to the other electron in either the d_{yz} or d_{zx} orbital forming a spin $S = 1$. These spins are arranged ferromagnetically along the c axis and antiferromagnetically in the ab plane (C-type), while the d_{yz}/d_{zx}-OO is alternating in all three directions (G-type). As shown in Fig. 1(b), the SO and the OO transition temperatures referred to, respectively, as T_{SO} and T_{OO}, depend on an ionic radius of R, which controls a degree of the VO_6 octahedra tilting [15].

In this system where the spin and the orbital degrees of freedom are closely coupled, the SO provides an interesting laboratory for investigating the orbital dynamics. There are two reasons to treat the spin and the orbital unequally. One is that the spin has $S = 1$, while the orbital pseudospin $T = 1/2$ reflecting the two possible states d_{yz} and d_{zx}. This means that the quantum fluctuation of the orbital is stronger than that of the spin. The other reason is that an exchange interaction is three dimensional (3D) for spins, while it is quasi-1D for orbitals in the C-type spin ordered state. This is due to the destructive interference of various orbital exchange processes [9]. Therefore the spin can be regarded as a classical variable forming a 3D long-range order, offering a quasi-1D model for the orbital dynamics, which has recently been investigated in terms of a spin wave approximation for the orbital pseudospin [16]. Below we report an experimental and theoretical study on the Raman scattering spectra in this quasi-1D orbital system. We adopted $LaVO_3$ and $NdVO_3$ as the prototypical system with the C-type SO and the G-type OO in RVO_3.

In Fig. 1(d), we show Raman spectra at various temperatures in $y(zz)\bar{y}$ and $y(xx)\bar{y}$ polarizations for $NdVO_3$ single crystal grown by the floating zone method [17,18]. Optical axes, x, y, and z, are taken parallel to the crystal axes, $a + b$, $a - b$, and c. At room T phonon modes are observed in $NdVO_3$. The Raman bands around 35 and 54 meV are assigned to oxygen bending and JT modes, respectively. Below T_{OO} ($= 188$ K), an additional peak due to an oxygen stretching mode [indicated by an open tri-

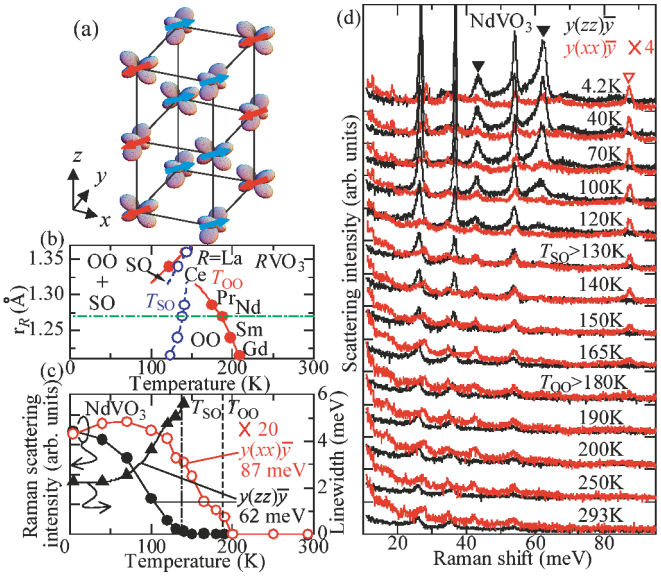

FIG. 1 (color). (a) Structure of C-type SO and G-type OO in RVO_3. Arrows and lobes indicate spins, and occupied d_{yz} or d_{zx} orbitals on V^{3+}, respectively. (b) Spin-orbital phase diagram of RVO_3. Closed and open circles indicate transition temperatures, T_{OO} and T_{SO}, respectively. (c) T dependence of the integrated Raman intensity of the peak around 87 meV in $y(xx)\bar{y}$ polarization (open circles) and that around 62 meV in $y(zz)\bar{y}$ (closed circles) for $NdVO_3$. Closed triangles indicate the T-dependent linewidth of the 62 meV band, which was estimated by the Fano model [14]. (d) Raman spectra for $y(zz)\bar{y}$ and $y(xx)\bar{y}$ configurations at various T in $NdVO_3$ with the exciting photon energy of 1.96 eV. The 43 and 62 meV peaks in $y(zz)\bar{y}$, indicated by filled triangles, are assigned to the two-orbiton excitation, while the 87 meV one in $y(xx)\bar{y}$, by an open triangle, to the phonon mode activated by the OO.

angle in Fig. 1(d)] appears at 87 meV only in $y(xx)\bar{y}$ polarization. Below T_{OO}, all the phonon modes have the A_g symmetry in the $P2_1/a$ monoclinic form. The 87 meV Raman band (V-O stretching in its origin), which has the B_{1g} symmetry in the original $Pbnm$ lattice, appears only in the monoclinic phase coupled with the G-type OO [15]. Below T_{SO} (=138 K), though $NdVO_3$ undergoes no structure phase transition at T_{SO}, new peaks emerge around 43 and 62 meV in $y(zz)\bar{y}$ Raman spectra, as indicated by closed triangles in Fig. 1(d). By excluding possibilities of phonon, charge, and magnetic excitations, or their multiparticle scatterings, we can conclude that these bands originate from orbital excitations, as we discuss in the following. (As for the general difficulty to distinguish the orbital excitation and the multiphonon mode, see also the controversy reported by the papers in Ref. [6].)

First, widths of the peaks are much broader than those of phonons, and the 62 meV band has a distinctly asymmetric shape. Any plausible combinations of the lower-lying phonon modes cannot account for the frequencies of these two bands, which excludes a possibility of two-(or multi-) phonon excitation as the origin of the Raman bands [19]. T dependence of the 62 meV band [see Fig. 1(c)] shows a clear difference from that of the 87 meV phonon band that stands for the OO induced lattice distortion [15]. The steep rise of the 62-meV-band intensity below T_{SO} indicates that this (as well as the 43 meV) band is inherent to both the spin- and the orbital-ordered state. Moreover, the 62-meV-band linewidth critically increases as T is increased towards T_{SO} [see Fig. 1(c)], while those of phonons are almost unchanged apart from conventional thermal broadening. These features imply that these two bands have a magnetic or an electronic origin. Second, charge excitations cannot be responsible for these bands, because the lowest Mott-Hubbard gap energy is too large ($\sim$2 eV), as described later. Third, magnon excitations are almost gapless and the observed peak energies are too high to ascribe to those. Furthermore, in the C-type SO state which has a ferromagnetic order along the c axis, two-magnon scattering is prohibited in the $y(zz)\bar{y}$ configuration [20]. In addition, both the softening and the broadening are expected to be observed in the two-magnon spectra. In the case of RVO_3, however, the 62 meV band broadens but does not soften towards T_{SO}. This behavior also indicates that the 62 meV band does not originate from two-magnon. Therefore, we can assign the origin of the Raman bands to orbital excitations. The JT mode around 54 meV is discerned from high T, and the intensity is enhanced together with the bands between 43 and 62 meV as T is lowered. This implies that the JT phonon is coupled with these Raman bands which have been assigned to orbital excitations.

To obtain further insight into the nature of the orbital excitations, it is important to consider a resonance with the Mott-Hubbard gap transition. Figure 2(a) presents optical conductivity spectra for $\mathbf{E} \parallel c$ at 10 K in $LaVO_3$ and $NdVO_3$. The Mott-Hubbard gap transition is observed as a distinct peak around 1.9 eV in this spin- and orbital-ordered phase in RVO_3. In the photoexcitation process below T_{SO} and T_{OO}, an electron can hop only between the d_{yz} or d_{zx} orbitals on the neighboring V sites along the c axis via the π bonding with the O $2p_y$ or $2p_x$ state, as

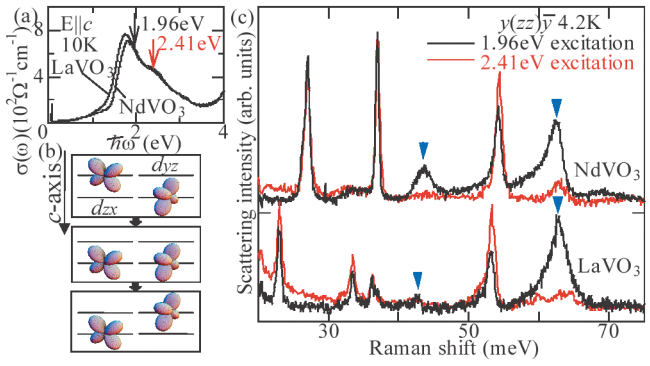

FIG. 2 (color). (a) Optical conductivity spectra for $\mathbf{E} \parallel c$ at 10 K in $NdVO_3$ and $LaVO_3$. (b) Two-orbiton Raman process in staggered orbital chain with ferromagnetic spin order. (c) Raman spectra at 4.2 K in $NdVO_3$ and $LaVO_3$ with the exciting photon energies of 1.96 and 2.41 eV (from He-Ne and Ar^+ lasers). The triangles indicate the peaks due to two-orbiton.

shown in the top and middle panels of Fig. 2(b) [9,21]. The d_{yz}-d_{yz} transition energy should be nearly equal to the d_{zx}-d_{zx} one.

The broad Raman bands around 43 and 62 meV show a remarkable resonance with this Mott-Hubbard gap transition. Figure 2(c) represents a comparison between the Raman scattering spectra in $NdVO_3$ and $LaVO_3$ at 4.2 K observed with two exciting photon energies of 1.96 and 2.41 eV. The 43 and 62 meV bands are distinctly enhanced for the photon energy of 1.96 eV which is almost equal to the energy of the orbital-dependent Mott-Hubbard gap transitions as discussed above. Therefore, it is reasonable to consider that this resonant Raman process involves the Mott-Hubbard gap transition as the intermediate state [the middle panel of Fig. 2(b)]. Interacting with the second photon, the d_{yz} (d_{zx}) electron returns to the original V site. In the final state of this Raman process, the orbital occupancy of the adjacent V sites along the c axis can be exchanged as compared with that of the initial state. We call this excitation *two-orbiton* by analogy with two-magnon.

The orbital excitation observed in the Raman spectra can be theoretically elucidated in terms of the following 1D Heisenberg model for orbital pseudospin [9,16]:

$$\mathcal{H} = \sum_i [J\vec{\tau}_i \cdot \vec{\tau}_{i+1} - \sqrt{8E_{\mathrm{DJT}}\omega_{\mathrm{ph}}}(\tau_i^z - \langle\tau_i^z\rangle)Q_i + \omega_{\mathrm{ph}}(P_i^2 + Q_i^2)/2 - 8E_{\mathrm{CJT}}\langle\tau_i^z\rangle\tau_i^z]. \quad (1)$$

Here, $\vec{\tau}_i$ is the pseudospin operator in the representation where d_{yz} and d_{zx} occupations correspond to $\tau^z = 1/2$ and $-1/2$, respectively. Q_i and P_i represent the E_v JT coordinate and its conjugate momentum for the octahedron centered at the V site i. ω_{ph} and E_{DJT} are a frequency and a relaxation energy of this JT phonon, respectively. In the last term of Eq. (1), we have taken into account a mean field $\langle\tau_i^z\rangle$ corresponding to static JT distortion with its relaxation energy E_{CJT} which appears due to 3D interchain coupling. It has been known that elementary excitations of this 1D antiferromagnetic Heisenberg model are described in terms of fermions with $T = 1/2$, which we refer to as *pseudospinons* in the present context. Therefore, we represent the model Eq. (1) in terms of the Jordan-Wigner spinless fermions [22] instead of the Holstein-Primakoff bosons [16]. We then employ the fully self-consistent random phase approximation (RPA), which guarantees the absence of long-range order in one dimension (at finite T in the case of $E_{\mathrm{CJT}} = 0$). In reality, however, three dimensionality of both orbital exchange interaction and phonon dispersion causes a 3D orbital long-range order accompanied by the JT distortion. We treat this effect by assuming a finite value of the staggered orbital order parameter $\langle\tau_i^z\rangle = (-1)^i\bar{\tau}$ satisfying self-consistent equations.

For the moment, we consider only the classical JT effects and take $E_{\mathrm{DJT}} = 0$. The inset of Fig. 3 shows the spectral density of the pseudospinon excitations with a red density corresponding to the intensity (for comparison, its dispersion obtained for $E_{\mathrm{CJT}} = 0$ is shown as a black curve). This finite value of $\bar{\tau}$ creates a gap in pseudospinon excitations via the last term in Eq. (1). This gap increases with increasing E_{CJT}. With $E_{\mathrm{CJT}}/J = 0.15$, a ratio of the low-energy band edge to the higher-energy one is approximately $2/3$, which corresponds to the ratio of the lower and upper peaks of the two-orbiton Raman bands. We take $J = 17.5$ meV which is comparable to the value chosen in a previous estimate by Motome *et al.* [9]. As the two-orbiton Raman scattering intensity of the $y(zz)\bar{y}$ polarization, we calculate the quantity, $\mathrm{Im}\int_0^\infty dt\langle(\sum_i\vec{\tau}_i(t)\cdot\vec{\tau}_{i+1}(t))\times(\sum_i\vec{\tau}_i(0)\cdot\vec{\tau}_{i+1}(0))\rangle e^{i\omega t}$. In the pseudospinon representation, particle-hole excitations give a dominant contribution to the Raman spectra as presented by a blue curve in Fig. 3(a). The higher-energy peak has much larger intensity than the lower-energy one, in contrast to a simple convolution of pseudospinon band (a black dashed curve). This is because in a convolution of pseudospinons for the Raman spectrum, there appears a form factor of $\cos^2 k$ which vanishes at $k = \pi/2$ corresponding to the lower-energy edge.

Next we turn on the dynamical JT coupling. Introducing a small value $E_{\mathrm{DJT}}/J = 0.01$ modifies the Raman spectra from the blue curve into the red one in Fig. 3(a). In the spectra, there also exist phonon contributions mediated and broadened by the pseudospinon excitations. They have a

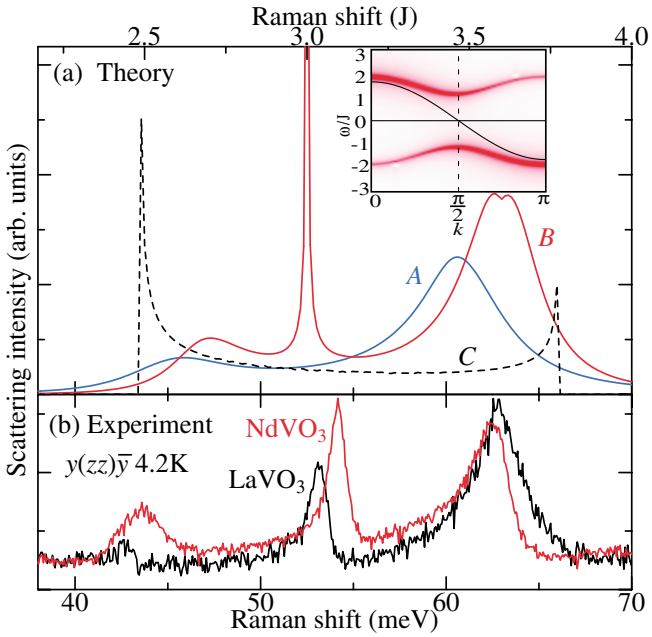

FIG. 3 (color). Comparison between the experimental and theoretical Raman spectra in RVO_3. (a) Theoretical results for the Raman spectra in static (A, $E_{\mathrm{CJT}}/J = 0.15$, $E_{\mathrm{DJT}}/J = 0$) and dynamical Jahn-Teller case (B, $E_{\mathrm{CJT}}/J = 0.15$, $E_{\mathrm{DJT}}/J = 0.01$), and for simple particle-hole excitation spectra of pseudospinons (C). The inset is a density plot for the pseudospinon excitation spectra, where the red density represents the intensity of the spectra. For comparison, a pseudospinon dispersion in the case of $E_{\mathrm{CJT}} = 0$ is shown by a black curve. For the definition of J, E_{CJT} and E_{DJT}, see Eq. (1) in text. (b) Experimental spectra in $y(zz)\bar{y}$ polarization for $NdVO_3$ and $LaVO_3$ at 4.2 K between 38 and 70 meV to be compared with the red curve B in the (a).

significant structure around ω_{ph} which appears as a middle peak of the red curve in Fig. 3(a). At the lowest T, these theoretical results show a remarkable agreement with experimental ones, as shown in Fig. 3(b). The difference between $LaVO_3$ and $NdVO_3$ can also be explained by a narrower bandwidth (smaller J) and a larger static JT effect for $NdVO_3$ which shows a larger VO_6 tilting [23].

Approaching to T_{SO}, the two-orbiton Raman band shows obvious broadening but no significant softening. This implies that the magnitude of the local order parameter/gap remains large even near T_{SO}, while the phase coherence is destroyed by spin fluctuation. This feature is beyond a simple mean-field-/RPA picture, where a softening of the two-orbiton energy occurs towards the phase transition. Because the Raman spectra are more sensitive to the local amplitude of the order parameter, the two-orbiton peak energy is expected to remain almost unchanged while the spectral shape gets broader and broader toward the low-energy side. The lower bound energy of this broadened spectrum corresponds to the mean-field order parameter, which shows softening near T_{SO}, but this is rather difficult to observe experimentally. To describe the T dependence appropriately, we should study a model including the spin degrees of freedom with a more elaborated method, which is left for future investigations.

In conclusion, we have found the orbital excitation bands, assigned to the two-orbiton process, in the resonant Raman scattering spectra for perovskite-type $LaVO_3$ and $NdVO_3$ with spin and orbital ordering of t_{2g} electrons. The orbiton excitation shows a unique highly quantum-mechanical nature that arises from the quasi-1D orbital chain with antiferroic orbital exchange interaction. The theoretical calculation based on the pseudospinon (fermion) approach taking full account of static or dynamic JT interaction can almost quantitatively reproduce the experimentally observed feature. The orbiton excitations as observed in the present study should be ubiquitous, although sometimes difficult to distinguish from phonons, in Mott insulators of transition-metal oxide, and play an important role in dynamics of the Mott transition in the light of melting of orbital order.

We thank S. Ishihara, Y. Motome, and B. Keimer for helpful discussions.

[1] *Physical Properties of High Temperature Superconductors*, edited by D. M. Ginzburg (World Scientific, Singapore, 1992), Vol. 3.
[2] *Colossal Magnetoresistive Oxides*, Advances in Condensed Matter Science Vol. 2, edited by Y. Tokura (Gordon and Breach, Amsterdam, 2000).
[3] P. W. Anderson, Mater. Res. Bull. **8**, 153 (1973).
[4] P. Fazekas and P. W. Anderson, Philos. Mag. **30**, 423 (1974).
[5] Y. Tokura and N. Nagaosa, Science **288**, 462 (2000).
[6] E. Saitoh *et al.*, Nature (London) **410**, 180 (2001); concerning the controversy about the orbiton interpretation, see also M. Grüninger *et al.*, Nature (London) **418**, 39 (2002); E. Saitoh *et al.*, Nature (London) **418**, 40 (2002).
[7] B. Keimer *et al.*, Phys. Rev. Lett. **85**, 3946 (2000).
[8] G. Khaliullin, P. Horsch, and A. M. Oleś, Phys. Rev. Lett. **86**, 3879 (2001).
[9] Y. Motome *et al.*, Phys. Rev. Lett. **90**, 146602 (2003).
[10] V. G. Zubkov, G. V. Bazuev, and G. P. Shveikin, Sov. Phys. Solid State **15**, 1079 (1973).
[11] M. Noguchi *et al.*, Phys. Rev. B **62**, 9271 (2000).
[12] G. R. Blake *et al.*, Phys. Rev. Lett. **87**, 245501 (2001).
[13] P. Bordet *et al.*, J. Solid State Chem. **106**, 253 (1993).
[14] U. Fano, Phys. Rev. **124**, 1866 (1961).
[15] S. Miyasaka *et al.*, Phys. Rev. B **68**, 100406 (2003).
[16] S. Ishihara, Phys. Rev. B **69**, 075118 (2004).
[17] S. Miyasaka, T. Okuda, and Y. Tokura, Phys. Rev. Lett. **85**, 5388 (2000).
[18] No additional electronic Raman band is discerned in the spectra for other polarizations except for the originally active phonon ones.
[19] Any combinations of Raman and infrared phonon modes cannot reproduce the Raman shift of the 62 meV band. As for the 43 meV mode, twice of the frequency (22 meV) for the infrared-active external mode (corresponding to rare-earth ion motion) is rather close. However, such a mode couples most weakly with electronic states of V atoms. It is not reasonable to assume that only the two-phonon band of the rare-earth mode could be sensitively activated only below T_{SO}. The 43 meV mode is also observed in the C-type spin- and G-type orbital-ordered state of YVO_3 (see Ref. [20]), where the twofold frequency of the rare-earth mode shows no more coincidence.
[20] In the C-type spin- and the G-type orbital-ordered phase in YVO_3, we observed broad Raman bands around 43 and 62 meV in addition to the sharp phonon bands at 34, 41, and 58 meV. As the ionic size of the R site is decreased from La to Y, the Raman shifts of the phonon increases systematically, while those of the peaks around 43 and 62 meV are almost unchanged. In contrast to the almost constant value of the Raman shift of these peaks, the dispersion of the spin wave in $LaVO_3$ is quite different from that in YVO_3. [C. Ulrich *et al.*, Phys. Rev. Lett. **91**, 257202 (2003); B. Keimer (unpublished)]. The R dependence of the Raman shift suggests that the Raman bands around 43 and 62 meV are not caused by the phonons, magnons, nor related excitations.
[21] S. Miyasaka, Y. Okimoto, and Y. Tokura, J. Phys. Soc. Jpn. **71**, 2086 (2002).
[22] E. Fradkin, *Field Theories of Condensed Matter Systems* (Addison-Wesley, Redwood City, CA, 1991).
[23] As seen in Fig. 3(b), the asymmetry of the 62 meV band in $LaVO_3$ is smaller than that in $NdVO_3$. The spectral shape of the two-orbiton depends not only on the particle-hole excitation spectra for pseudospinons but also on the energies of the JT effect and the exchange interaction in Eq. (1). By increasing the ionic size of the R site in RVO_3 up to La, the tilting of VO_6 octahedra is decreased, while the orbital exchange interaction is enhanced. Because of the large orbital exchange interaction, the linewidth of the two-orbiton in $LaVO_3$ is broader than that in $NdVO_3$, and consequently the asymmetry of the 62 meV band may hardly be observed in $LaVO_3$.